Article

Effect of Side Chains on Turns and Helices in Peptides of β-Aminoxy Acids

Dan Yang, Yu-Hui Zhang, Bing Li, Dan-Wei Zhang, Jenny Chun-Yu Chan, Nian-Yong Zhu, Shi-Wei Luo, and Yun-Dong Wu

J. Am. Chem. Soc., **2004**, 126 (22), 6956-6966• DOI: 10.1021/ja049976s • Publication Date (Web): 12 May 2004

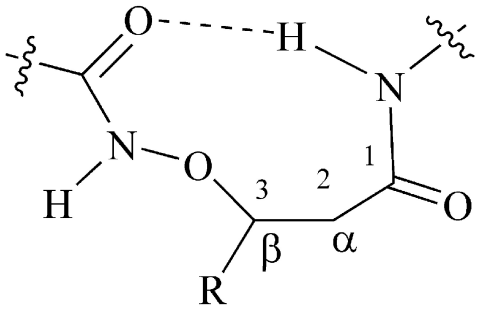

R = Me, Et, COOBn, $CH_2CH_2CH{=}CH_2$, *i*-Bu, *i*-Pr

β^3-aminoxy peptides

More About This Article

Additional resources and features associated with this article are available within the HTML version:

- Supporting Information
- Links to the 2 articles that cite this article, as of the time of this article download
- Access to high resolution figures
- Links to articles and content related to this article
- Copyright permission to reproduce figures and/or text from this article

View the Full Text HTML

J|A|C|S
ARTICLES
Published on Web 05/12/2004

Effect of Side Chains on Turns and Helices in Peptides of β^3-Aminoxy Acids

Dan Yang,*[,†,§] Yu-Hui Zhang,[†] Bing Li,[†] Dan-Wei Zhang,[§] Jenny Chun-Yu Chan,[†] Nian-Yong Zhu,[†] Shi-Wei Luo,[‡] and Yun-Dong Wu*[,‡]

Contribution from the Department of Chemistry, The University of Hong Kong, Pokfulam Road, Hong Kong, China, Department of Chemistry, The Hong Kong University of Science and Technology, Clear Water Bay, Kowloon, Hong Kong, China, and Department of Chemistry, Fudan University, Shanghai, China

Received January 1, 2004; E-mail: yangdan@hku.hk

Abstract: We have investigated, using NMR, IR, and CD spectroscopy and X-ray crystallography, the conformational properties of peptides **1**−**10** of β^3-aminoxy acids ($NH_2OCHRCH_2COOH$) having different side chains on the β carbon atom (e.g., R = Me, Et, COOBn, $CH_2CH_2CH{=}CH_2$, *i*-Bu, *i*-Pr). The β N−O turns and β N−O helices that involve a nine-membered-ring intramolecular hydrogen bond between NH_{i+2} and CO_i, which have been found previously in peptides of $\beta^{2,2}$-aminoxy acids ($NH_2OCH_2CMe_2COOH$), are also present in those β^3-aminoxy peptides. X-ray crystal structures and NMR spectral analysis reveal that, in the β N−O turns and β N−O helices induced by β^3-aminoxy acids, the N−O bond could be either anti or gauche to the C_α−C_β bond depending on the size of the side chain; in contrast, only the anti conformation was found in $\beta^{2,2}$-aminoxy peptides. Both diamide **1** and triamide **9** exist in different conformations in solution and in the solid state: parallel sheet structures in the solid state and predominantly β N−O turn and β N−O helix conformations in nonpolar solvents. Theoretical studies on a series of model diamides rationalize very well the experimentally observed conformational features of these β^3-aminoxy peptides.

Introduction

The side chains of individual residues play important roles in the formation and stability of secondary structures in peptides comprising α-amino acids. It is well known that some amino acids, such as leucine and alanine, have higher propensities than others for forming α-helices.[1−10] Interactions between side chains, including salt bridges,[11−16] hydrogen bonds,[11,12,17,18] and aromatic and hydrophobic interactions,[19−30] also have important effects on the folding of α-helices. The addition of one more α-substituent to α-amino acids leads to acyclic or cyclic α,α-disubstituted amino acids, which strongly promote the formation of 3_{10} or α-helices, even in small oligopeptides.[31−35]

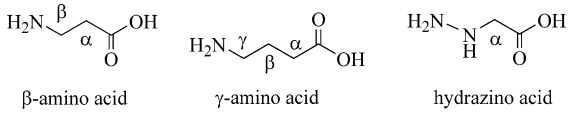

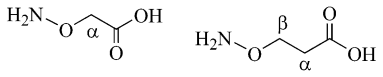

For β-peptides, that is, peptides of β-amino acids, the formation of secondary structures is also dependent on the

† The University of Hong Kong.
‡ The Hong Kong University of Science and Technology.
§ Fudan University.

(1) Yang, J. X.; Spek, E. J.; Gong, Y. X.; Zhou, H. X.; Kallenbach, N. R. *Protein Sci.* **1997**, *6*, 1264−1272.
(2) Rohl, C. A.; Chakrabartty, A.; Baldwin, R. L. *Protein Sci.* **1996**, *5*, 2623−2637.
(3) Blaber, M.; Zhang, X. J.; Lindstrom, J. D.; Pepiot, S. D.; Baase, W. A.; Matthews, B. W. *J. Mol. Biol.* **1994**, *235*, 600−624.
(4) Park, S. H.; Shalongo, W.; Stellwagen, E. *Biochemistry* **1993**, *32*, 7048−7053.
(5) Lyu, P. C.; Sherman, J. C.; Chen, A.; Kallenbach, N. R. *Proc. Natl. Acad. Sci. U.S.A.* **1991**, *88*, 5317−5320.
(6) Scholtz, J. M.; York, E. J.; Stewart, J. M.; Baldwin, R. L. *J. Am. Chem. Soc.* **1991**, *113*, 5102−5104.
(7) Lyu, P. C.; Liff, M. I.; Marky, L. A.; Kallenbach, N. R. *Science* **1990**, *250*, 669−673.
(8) Oneil, K. T.; Degrado, W. F. *Science* **1990**, *250*, 646−651.
(9) Marqusee, S.; Robbins, V. H.; Baldwin, R. L. *Proc. Natl. Acad. Sci. U.S.A.* **1989**, *86*, 5286−5290.
(10) Padmanabhan, S.; Marqusee, S.; Ridgeway, T.; Laue, T. M.; Baldwin, R. L. *Nature* **1990**, *344*, 268−270.
(11) Huyghues-Despointes, B. M. P.; Baldwin, R. L. *Biochemistry* **1997**, *36*, 1965−1970.
(12) Scholtz, J. M.; Qian, H.; Robbins, V. H.; Baldwin, R. L. *Biochemistry* **1993**, *32*, 9668−9676.
(13) Huyghues-Despointes, B. M. P.; Scholtz, J. M.; Baldwin, R. L. *Protein Sci.* **1993**, *2*, 80−85.
(14) Merutka, G.; Stellwagen, E. *Biochemistry* **1991**, *30*, 1591−1594.
(15) Lyu, P. C.; Marky, L. A.; Kallenbach, N. R. *J. Am. Chem. Soc.* **1989**, *111*, 2733−2734.
(16) Marqusee, S.; Baldwin, R. L. *Proc. Natl. Acad. Sci. U.S.A.* **1987**, *84*, 8898−8902.
(17) Stapley, B. J.; Doig, A. J. *J. Mol. Biol.* **1997**, *272*, 465−473.
(18) Huyghues-Despointes, B. M. P.; Klingler, T. M.; Baldwin, R. L. *Biochemistry* **1995**, *34*, 13267−13271.
(19) Aravinda, S.; Shamala, N.; Das, C.; Sriranjini, A.; Karle, I. L.; Balaram, P. *J. Am. Chem. Soc.* **2003**, *125*, 5308−5315.
(20) Shi, Z. S.; Olson, C. A.; Kallenbach, N. R. *J. Am. Chem. Soc.* **2002**, *124*, 3284−3291.
(21) Andrew, C. D.; Bhattacharjee, S.; Kokkoni, N.; Hirst, J. D.; Jones, G. R.; Doig, A. J. *J. Am. Chem. Soc.* **2002**, *124*, 12706−12714.
(22) Olson, C. A.; Shi, Z. S.; Kallenbach, N. R. *J. Am. Chem. Soc.* **2001**, *123*, 6451−6452.
(23) Minoux, H.; Chipot, C. *J. Am. Chem. Soc.* **1999**, *121*, 10366−10372.
(24) Gallivan, J. P.; Dougherty, D. A. *Proc. Natl. Acad. Sci. U.S.A.* **1999**, *96*, 9459−9464.

10.1021/ja049976s CCC: $27.50

structures of the individual residues. β-Peptides having a variety of different substitution patterns can adopt distinct helical structures.[36−38] The 14-helix, which contains a 14-membered-ring hydrogen bond between N−H_i and C═O_{i+2} groups, has been observed in β-peptides consisting of β^2-, β^3-, or acyclic $\beta^{2,3}$-amino acids.[39−50] β-Peptides comprising *trans*-2-aminocyclohexanecarboxylic acid (ACHC) residues, a constrained cyclic amino acid, also favor 14-helix formation; the cyclohexane rings on the peptide backbone are believed to contribute to the stability of this 14-helix.[51−56] Another helical conformation, the 12-helix, is, however, preferred by β-peptides having cyclopentane rings on their backbones.[54,57−65] β-Peptides with alternating β^2- and β^3-amino acid residues display a "12/10/12 helix", which is characterized by intertwined 12- and 10-membered-ring hydrogen bonds.[66,67] Building β-peptides with a backbone constrained by *cis*-disubstituted oxetane rings leads to an unprecedented 10-helix.[68] The 8-helix, with hydrogen bonding between adjacent amino acid residues, can be found in cyclopropane-constrained β-peptides[69] and in acyclic $\beta^{2,3}$-peptides having a hydroxyl group in the 2-position of the backbone.[70] In contrast to the intensive research on β-peptides, γ-peptides have received far less attention. Only the 14-helix conformation has been found in acyclic γ^4-, $\gamma^{2,4}$-, and $\gamma^{2,3,4}$-peptides.[71−75]

Replacing the carbon atoms in a peptide's backbone with heteroatoms represents an interesting approach toward identifying new classes of foldamers. Replacing the β-carbon atom of β-amino acid residues in β-peptides with a nitrogen atom has led to the discovery of new kinds of foldamers, hydrazino peptides, which were reported by Grel and Hofmann et al.[76,77] We are interested in determining the secondary structures of peptides composed of α- and β-aminoxy acids in which the β-carbon atom of β-amino acids and the γ-carbon atom of γ-amino acids, respectively, have been replaced by oxygen atoms. Previously, we reported that the α N−O turn (involving an eight-membered-ring intramolecular hydrogen bond) and 1.8_8 helix conformations observed in peptides of α-aminoxy acids are independent of their side chains.[78−82] Recently, oligomers constructed from $\beta^{2,2}$-aminoxy acids have been demonstrated to adopt novel 1.7_9-helices consisting of consecutive N−O turns, each featuring a nine-membered-ring intramolecular hydrogen bond (referred to as a "β N−O turn").[83]

Backbone torsional angles are usually used to analyze the conformations of peptides (Figure 1A). The torsional angles ϕ and ψ of α-helix backbones in α-peptides have repeating values near the canonical values of −60° and −40°, respectively. For β-peptides, helical conformations always require a gauche orientation with respect to the torsional angle θ defined by the $C_\alpha-C_\beta$ bond (Figure 1B).[36] The 14-helix formed by γ-peptides adopts a gauche conformation with respect to the dihedral angle

(25) Fernandez Recio, J.; Vazquez, A.; Civera, C.; Sevilla, P.; Sancho, J. *J. Mol. Biol.* **1997**, *267*, 184−197.
(26) Wouters, J. *Protein Sci.* **1998**, *7*, 2472−2475.
(27) Viguera, A. R.; Serrano, L. *Biochemistry* **1995**, *34*, 8771−8779.
(28) Stapley, B. J.; Rohl, C. A.; Doig, A. J. *Protein Sci.* **1995**, *4*, 2383−2391.
(29) Padmanabhan, S.; Baldwin, R. L. *J. Mol. Biol.* **1994**, *241*, 706−713.
(30) Padmanabhan, S.; Baldwin, R. L. *Protein Sci.* **1994**, *3*, 1992−1997.
(31) Venkatraman, J.; Shankaramma, S. C.; Balaram, P. *Chem. Rev.* **2001**, *101*, 3131−3152.
(32) Karle, I. L. *Acc. Chem. Res.* **1999**, *32*, 693−701.
(33) Kaul, R.; Balaram, P. *Bioorg. Med. Chem.* **1999**, *7*, 105−117.
(34) Karle, I. L.; Balaram, P. *Biochemistry* **1990**, *29*, 6747−6756.
(35) Toniolo, C.; Crisma, M.; Formaggio, F.; Peggion, C. *Biopolymers* **2001**, *60*, 396−419.
(36) Cheng, R. P.; Gellman, S. H.; DeGrado, W. F. *Chem. Rev.* **2001**, *101*, 3219−3232.
(37) Gellman, S. H. *Acc. Chem. Res.* **1998**, *31*, 173−180.
(38) Seebach, D.; Matthews, J. L. *Chem. Commun.* **1997**, 2015−2022.
(39) Seebach, D.; Overhand, M.; Kuehnle, F. N. M.; Martinoni, B. *Helv. Chim. Acta* **1996**, *79*, 913−941.
(40) Seebach, D.; Ciceri, P. E.; Overhand, M.; Jaun, B.; Rigo, D.; Oberer, L.; Hommel, U.; Amstutz, R.; Widmer, H. *Helv. Chim. Acta* **1996**, *79*, 2043−2066.
(41) Seebach, D.; Abele, S.; Gademann, K.; Guichard, G.; Hintermann, T.; Jaun, B.; Matthews, J. L.; Schreiber, J. V.; Oberer, L.; Hommel, U.; Widmer, H. *Helv. Chim. Acta* **1998**, *81*, 932−982.
(42) Seebach, D.; Schreiber, J. V.; Abele, S.; Daura, X.; van Gunsteren, W. F. *Helv. Chim. Acta* **2000**, *83*, 34−57.
(43) Seebach, D.; Jacobi, A.; Rueping, M.; Gademann, K.; Ernst, M.; Jaun, B. *Helv. Chim. Acta* **2000**, *83*, 2115−2140.
(44) Arvidsson, P. I.; Rueping, M.; Seebach, D. *Chem. Commun.* **2001**, 649−650.
(45) Etezady-Esfarjani, T.; Hilty, C.; Wuethrich, K.; Rueping, M.; Schreiber, J.; Seebach, D. *Helv. Chim. Acta* **2002**, *85*, 1197−1209.
(46) Seebach, D.; Mahajan, Y. R.; Senthilkumar, R.; Rueping, M.; Jaun, B. *Chem. Commun.* **2002**, 1598−1599.
(47) Hintermann, T.; Seebach, D. *Synlett* **1997**, 437−438.
(48) Raguse, T. L.; Lai, J. R.; Gellman, S. H. *Helv. Chim. Acta* **2002**, *85*, 4154−4164.
(49) Hart, S. A.; Bahadoor, A. B. F.; Matthews, E. E.; Qiu, X. Y. J.; Schepartz, A. *J. Am. Chem. Soc.* **2003**, *125*, 4022−4023.
(50) Cheng, R. P.; DeGrado, W. F. *J. Am. Chem. Soc.* **2001**, *123*, 5162−5163.
(51) Appella, D. H.; Christianson, L. A.; Karle, I. L.; Powell, D. R.; Gellman, S. H. *J. Am. Chem. Soc.* **1996**, *118*, 13071−13072.
(52) Appella, D. H.; Barchi, J. J., Jr.; Durell, S. R.; Gellman, S. H. *J. Am. Chem. Soc.* **1999**, *121*, 2309−2310.
(53) Appella, D. H.; Christianson, L. A.; Karle, I. L.; Powell, D. R.; Gellman, S. H. *J. Am. Chem. Soc.* **1999**, *121*, 6206−6212.
(54) Barchi, J. J., Jr.; Huang, X.; Appella, D. H.; Christianson, L. A.; Durell, S. R.; Gellman, S. H. *J. Am. Chem. Soc.* **2000**, *122*, 2711−2718.
(55) Raguse, T. L.; Lai, J. R.; LePlae, P. R.; Gellman, S. H. *Org. Lett.* **2001**, *3*, 3963−3966.
(56) Raguse, T. L.; Lai, J. R.; Gellman, S. H. *J. Am. Chem. Soc.* **2003**, *125*, 5592−5593.
(57) Appella, D. H.; Christianson, L. A.; Klein, D. A.; Powell, D. R.; Huang, X.; Barchi, J. J., Jr.; Gellman, S. H. *Nature* **1997**, *387*, 381−384.
(58) Applequist, J.; Bode, K. A.; Appella, D. H.; Christianson, L. A.; Gellman, S. H. *J. Am. Chem. Soc.* **1998**, *120*, 4891−4892.
(59) Appella, D. H.; Christianson, L. A.; Klein, D. A.; Richards, M. R.; Powell, D. R.; Gellman, S. H. *J. Am. Chem. Soc.* **1999**, *121*, 7574−7581.
(60) Wang, X.; Espinosa, J. F.; Gellman, S. H. *J. Am. Chem. Soc.* **2000**, *122*, 4821−4822.
(61) Lee, H.-S.; Syud, F. A.; Wang, X.; Gellman, S. H. *J. Am. Chem. Soc.* **2001**, *123*, 7721−7722.
(62) LePlae, P. R.; Fisk, J. D.; Porter, E. A.; Weisblum, B.; Gellman, S. H. *J. Am. Chem. Soc.* **2002**, *124*, 6820−6821.
(63) Woll, M. G.; Fisk, J. D.; LePlae, P. R.; Gellman, S. H. *J. Am. Chem. Soc.* **2002**, *124*, 12447−12452.
(64) Porter, E. A.; Wang, X.; Schmitt, M. A.; Gellman, S. H. *Org. Lett.* **2002**, *4*, 3317−3319.
(65) Porter, E. A.; Wang, X. F.; Lee, H. S.; Weisblum, B.; Gellman, S. H. *Nature* **2000**, *404*, 565−565.
(66) Seebach, D.; Gademann, K.; Schreiber, J. V.; Matthews, J. L.; Hintermann, T.; Jaun, B.; Oberer, L.; Hommel, U.; Widmer, H. *Helv. Chim. Acta* **1997**, *80*, 2033−2038.
(67) Rueping, M.; Schreiber, J. V.; Lelais, G.; Jaun, B.; Seebach, D. *Helv. Chim. Acta* **2002**, *85*, 2577−2593.
(68) Claridge, T. D. W.; Goodman, J. M.; Moreno, A.; Angus, D.; Barker, S. F.; Taillefumier, C.; Watterson, M. P.; Fleet, G. W. J. *Tetrahedron Lett.* **2001**, *42*, 4251−4255.
(69) Abele, S.; Seiler, P.; Seebach, D. *Helv. Chim. Acta* **1999**, *82*, 1559−1571.
(70) Gademann, K.; Hane, A.; Rueping, M.; Jaun, B.; Seebach, D. *Angew. Chem., Int. Ed.* **2003**, *42*, 1534−1537.
(71) Hanessian, S.; Luo, X. H.; Schaum, R.; Michnick, S. *J. Am. Chem. Soc.* **1998**, *120*, 8569−8570.
(72) Hanessian, S.; Luo, X. H.; Schaum, R. *Tetrahedron Lett.* **1999**, *40*, 4925−4929.
(73) Hintermann, T.; Gademann, K.; Jaun, B.; Seebach, D. *Helv. Chim. Acta* **1998**, *81*, 983−1002.
(74) Seebach, D.; Brenner, M.; Rueping, M.; Schweizer, B.; Jaun, B. *Chem. Commun.* **2001**, 207−208.
(75) Seebach, D.; Brenner, M.; Rueping, M.; Jaun, B. *Chem.-Eur. J.* **2002**, *8*, 573−584.
(76) Cheguillaume, A.; Salaun, A.; Sinbandhit, S.; Potel, M.; Gall, P.; Baudy-Floc'h, M.; Le Grel, P. *J. Org. Chem.* **2001**, *66*, 4923−4929.
(77) Gunther, R.; Hofmann, H. J. *J. Am. Chem. Soc.* **2001**, *123*, 247−255.
(78) Yang, D.; Ng, F. F.; Li, Z. J.; Wu, Y. D.; Chan, K. W. K.; Wang, D. P. *J. Am. Chem. Soc.* **1996**, *118*, 9794−9795.
(79) Wu, Y. D.; Wang, D. P.; Chan, K. W. K.; Yang, D. *J. Am. Chem. Soc.* **1999**, *121*, 11189−11196.
(80) Yang, D.; Qu, J.; Li, B.; Ng, F. F.; Wang, X. C.; Cheung, K. K.; Wang, D. P.; Wu, Y. D. *J. Am. Chem. Soc.* **1999**, *121*, 589−590.
(81) Yang, D.; Li, B.; Ng, F. F.; Yan, Y. L.; Qu, J.; Wu, Y. D. *J. Org. Chem.* **2001**, *66*, 7303−7312.
(82) Yang, D.; Qu, J.; Li, W.; Zhang, Y. H.; Ren, Y.; Wang, D. P.; Wu, Y. D. *J. Am. Chem. Soc.* **2002**, *124*, 12410−12411.
(83) Yang, D.; Zhang, Y. H.; Zhu, N. Y. *J. Am. Chem. Soc.* **2002**, *124*, 9966−9967.

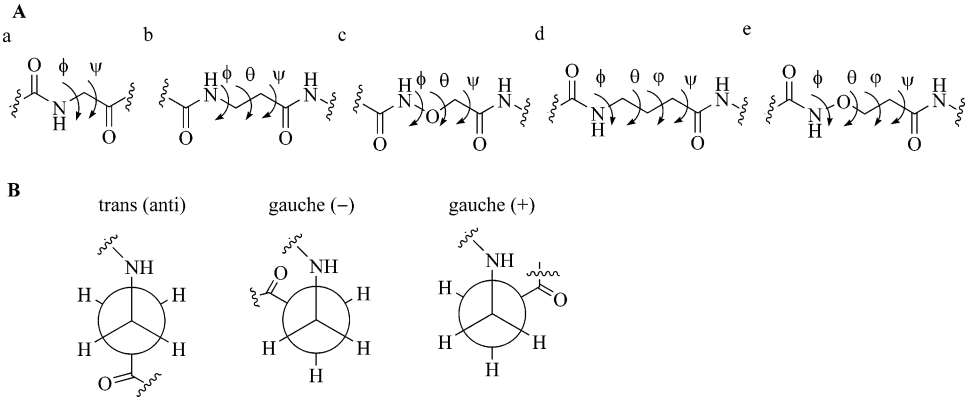

Figure 1. (A) Defining torsional angles in (a) α-peptides, (b) β-peptides, (c) α-aminoxy peptides, (d) γ-peptides, and (e) β-aminoxy peptides. (B) Rotamers of β-alanine with respect to the dihedral angle θ.

Chart 1

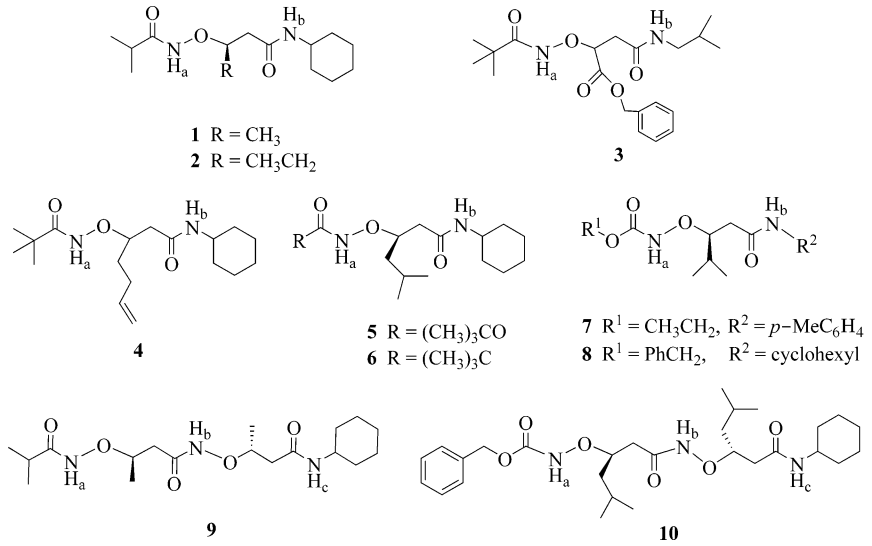

θ defined by the $C_\beta-C_\gamma$ bond.[71−75] For α N−O turns and 1.8_8 helices in peptides composed of α-aminoxy acids, gauche conformations are also favored with respect to the torsional angle θ defined by the O−C_α bond, rather than the $C_\alpha-C_\beta$ bond in β-peptides.[78−82] The crystal structures of $\beta^{2,2}$-aminoxy peptides indicate that β N−O turns and 1.7_9-helices all favor anti conformations, with dihedral angles θ (defined by the O−C_β bond) close to 170°.[83]

In comparison with α-aminoxy acids, the extra β-carbon atom in the backbone of β-aminoxy acids leads to greater variations in substitution patterns and results in considerable conformational flexibility. As a consequence, many more secondary structures are possible. Therefore, the following questions arise immediately: (1) Will the β N−O turn and helix observed in $\beta^{2,2}$-aminoxy peptides be maintained in other β-aminoxy peptides having different substitution patterns? (2) Will the nature of the side chains affect the conformations of those β-aminoxy peptides? To address these questions, we designed and synthesized a series of β^3-aminoxy peptides **1**−**10** having different side chains on the β-carbon atom (Chart 1). Here, we report conformational studies of those peptides along with a theoretical understanding of the conformational features.

Results and Discussion

Studying Diamides 1−5 and 7 by ^{1}H NMR Spectroscopy. Two ^{1}H NMR spectroscopy methods, (a) studying the concentration dependence of the chemical shifts of amide protons[84] and (b) the gradual addition of a strong hydrogen-bond acceptor (such as DMSO-d_6) to a dilute solution of the peptide in a non-hydrogen-bonding solvent (such as $CDCl_3$),[85] are commonly used to probe the formation of intramolecular hydrogen bonds by amide protons in linear peptides. We have applied these two methods to characterize the intramolecular hydrogen bonds present in the oligomers of β^3-aminoxy acids.

^{1}H NMR spectra of diamides **1**−**5** and **7** progressively diluted from 100 to 0.78 mM in $CDCl_3$ indicate that the *N*-oxy amide NH_a proton shifts upfield more significantly than does the amide NH_b proton at the C-terminus (Figure 2a provides an example of the dilution study using **1**).[86] The chemical shifts of both the NH_a and the NH_b protons remain constant at concentrations below 6 mM, which is a result of deaggregation. In addition, ^{1}H NMR spectra obtained upon adding DMSO-d_6 to solutions of **1**−**5** and **7** at 5 mM in $CDCl_3$ show that, with increasing amounts of DMSO-d_6, the signal of the NH_a proton shifts downfield dramatically ($\Delta\delta$ = 1.39−2.14 ppm) whereas the signal of the NH_b proton exhibits little change ($\Delta\delta$ = 0.18−0.64 ppm) (Figure 2b provides an example of the DMSO-d_6 addition study using **1**).[86] These results suggest that the *N*-oxy

(84) Haque, T. S.; Little, J. C.; Gellman, S. H. *J. Am. Chem. Soc.* **1994**, *116*, 4105−4106.
(85) Copeland, G. T.; Jarvo, E. R.; Miller, S. J. *J. Org. Chem.* **1998**, *63*, 6784−6785.
(86) See the Supporting Information.

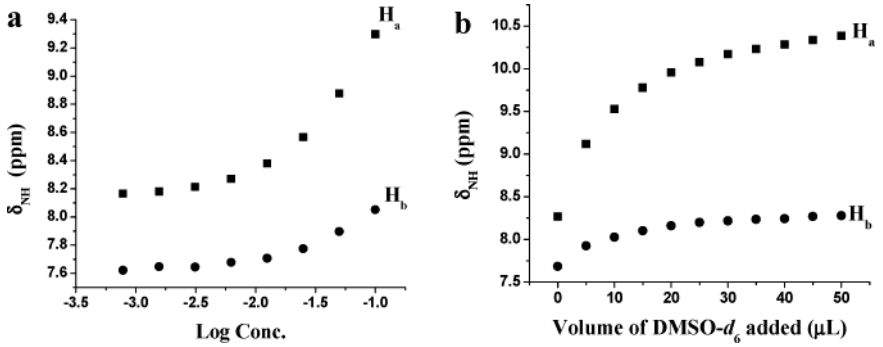

Figure 2. (a) Chemical shifts of amide protons as a function of the logarithm of the concentration of diamide **1** in $CDCl_3$ at room temperature. (b) Chemical shifts of amide protons as a function of the amount of DMSO-d_6 added in a solution of diamide **1** (5 mM) in $CDCl_3$ (0.5 mL at room temperature).

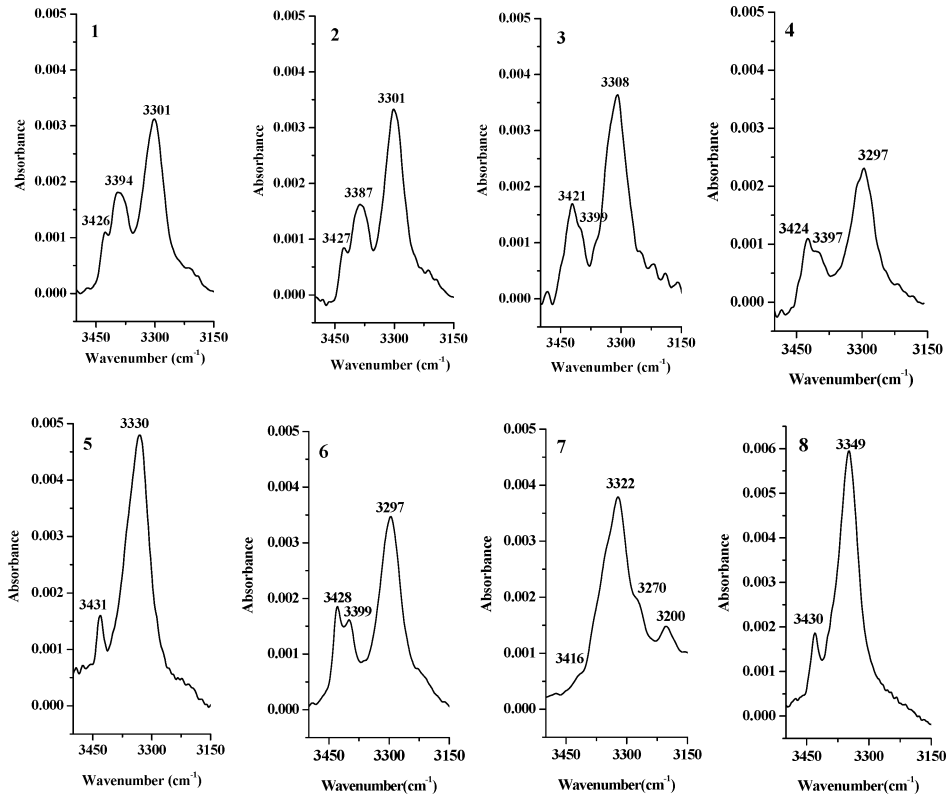

Figure 3. The N−H stretching region of FTIR spectra of diamides **1**−**8** at 2 mM in CH_2Cl_2 at room temperature after subtraction of the spectrum of pure CH_2Cl_2.

amide NH_a proton is solvent accessible and that the amide NH_b proton at the C-terminus is intramolecularly hydrogen-bonded. Therefore, the β N−O turns involving an intramolecular nine-membered-ring hydrogen bond that are found in $\beta^{2,2}$-aminoxy peptides are maintained in diamides **1**−**5** and **7** of β^3-aminoxy acids.

Studying Diamides 1−8 by IR Spectroscopy. The small abundance of non-hydrogen-bonded states cannot be determined from the ^{1}H NMR spectra because the equilibrium between the non-hydrogen-bonded and hydrogen-bonded states is usually rapid on the time scale of NMR spectroscopy. Thus, each observed value of δ_{NH} represents a population-weighted average of the contributing states. In contrast, the time scale of IR spectroscopic measurements is short enough to distinguish clearly the N−H stretching signals of hydrogen-bonded and non-hydrogen-bonded states. Therefore, data from the N−H stretching region of IR spectra provide insight into the degree of hydrogen bond formation in nonpolar solvents.

According to our previous studies,[78,81] the IR absorption of the non-hydrogen-bonded amide NH and *N*-oxy amide NH appeared in the region of 3450−3400 and 3340−3400 cm^{-1}, respectively, while the absorption peaks corresponding to the hydrogen-bonded normal amide NH and *N*-oxy amide NH appeared below 3370 and 3250 cm^{-1}, respectively.

Figure 3 presents the N−H stretching region of the FTIR spectra of diamides **1**−**8**. The spectra were recorded at a very low concentration (2 mM) at which intermolecular hydrogen bonding is unlikely to occur (Figure 2). We observe three major peaks for diamides **1**−**4** and **6**: the small N−H stretching bands at 3421−3428 cm^{-1} are assigned to the stretching of the non-hydrogen-bonded amide NH_b groups at the C-termini; the absorptions in the region 3387−3399 cm^{-1} correspond to the non-hydrogen-bonded *N*-oxy amide NH_a groups at the N-termini; the biggest peaks in the region 3297−3308 cm^{-1} are due to the stretching of the hydrogen-bonded C-terminal amide NH_b groups. For diamides **5**, **7**, and **8**, in addition to the small

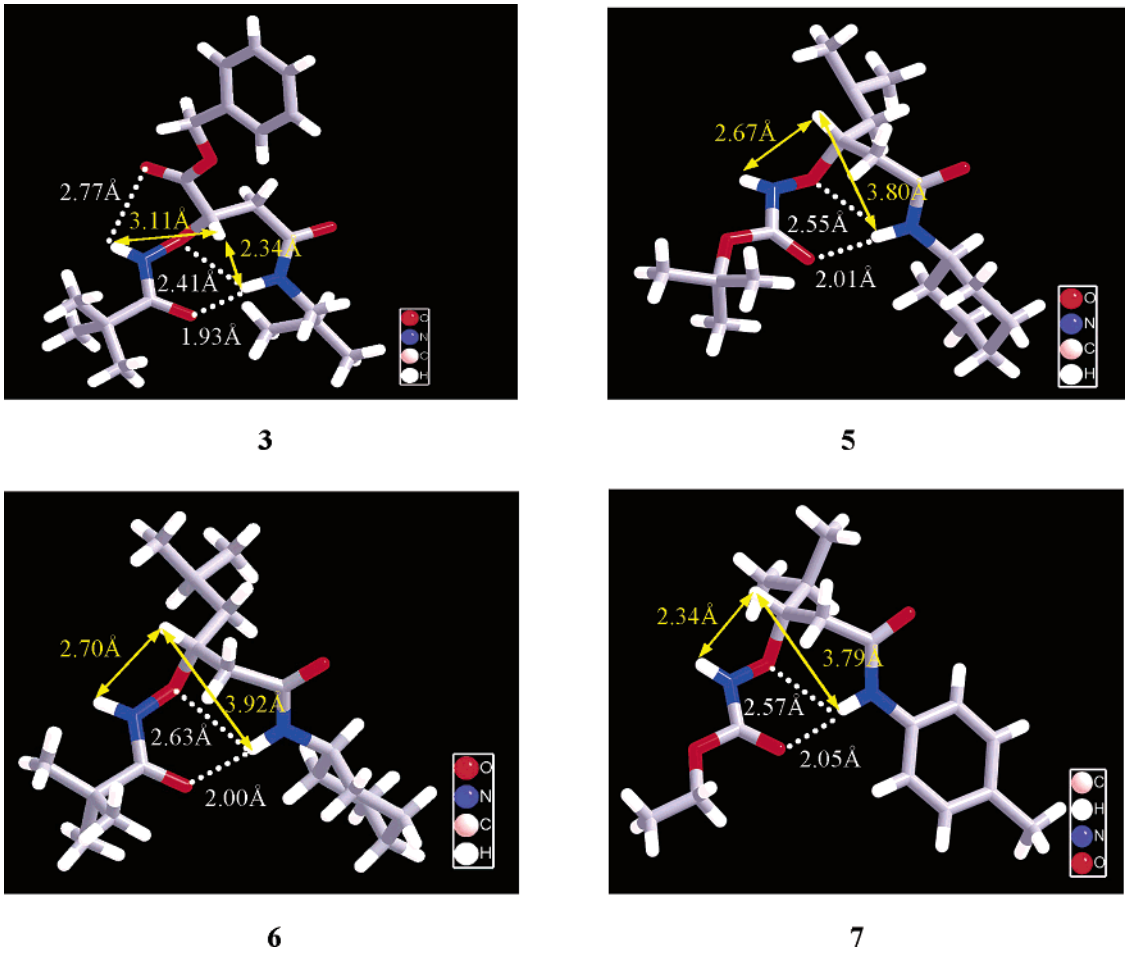

Figure 4. Solid-state structures of diamides **3**, **5**, **6**, and **7**.

peaks of the non-hydrogen-bonded NH_b groups at the C-termini (3431, 3416, and 3430 cm^{-1}, respectively), we assigned the broad peaks at 3330, 3322, and 3349 cm^{-1}, respectively, to the stretching of the hydrogen-bonded amide NH_b groups at the C-termini overlapped with those of the non-hydrogen-bonded carbamate NH_a groups at the N-termini. Two additional small peaks at 3270 and 3200 cm^{-1} in the spectrum of diamide **7** are due to the vibrational coupling of the C-terminal N−H unit with its adjacent aryl group.[81] The significantly larger populations of the hydrogen-bonded amide NH_b groups at the C-termini indicate that the nine-membered-ring hydrogen-bonded conformations of the β^3-aminoxy diamides **1**−**8** predominate in CH_2Cl_2 solutions.

X-ray Crystallographic Analysis of Two Types of β N−O Turns. We obtained samples of diamides **3** and **5**−**7** that were suitable for single-crystal X-ray structural analysis. The expected β N−O turns involving a nine-membered-ring hydrogen bond between the C═O_i and NH_{i+2} units, which are stabilized further by another six-membered-ring hydrogen bond between the NH_{i+2} and NO_{i+1} units, are observed in the crystal structures of all four compounds (Figure 4). There are significant differences, however, between the turns observed in **3** and those in **5**−**7**. In diamide **3** (Figure 4), the N−O bond of the β N−O turn is anti to the C_α−C_β bond, having a dihedral angle θ of 167.2°; the H···H distance between the NH_a and $C_\beta H$ units is 3.11 Å, which is longer than that between the NH_b and $C_\beta H$ units (2.34 Å). The torsional angles of **3** are comparable to those of the previously reported $\beta^{2,2}$-aminoxy peptide **18** (Table 1), but they are distinct from those of **5**, **6**, and **7**, in which the N−O bond is gauche to the C_α−C_β bond with dihedral angles θ of 73.8°, 70.42°, and 81.4°, respectively. The H···H distances between the NH_a and $C_\beta H$ units in the solid-state structures of **5**−**7** are ca. 2.7 Å and are shorter than those between the NH_b and $C_\beta H$ units (ca. 3.8 Å) (Figure 4). Taken together, we conclude that two types of β N−O turns, having anti and gauche conformations, respectively, about the θ dihedral angle, can occur for β^3-aminoxy peptides in the solid state and that the former is similar to the β N−O turns found in $\beta^{2,2}$-aminoxy peptides.

Table 1. Torsional Angles of Diamides **3**, **5**−**7**, and **18**[83] in Their Solid-State Structures

compound	ϕ	θ	φ	ψ
3	−97.76°	167.23°	−71.69°	9.80°
5	−120.67°	73.86°	75.19°	−71.60°
6	−115.85°	70.42°	77.49°	−70.10°
7	−123.69°	81.47°	70.52°	−77.33°
18[a]	−90.23°	172.83°	−64.97°	4.20°

[a] Structure of **18**:

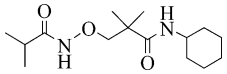

Studying Diamide 4 by ^{1}H NMR Spectroscopy. Interestingly, two sets of signals in 1:5 ratios are present for both the NH_a and the NH_b protons in the ^{1}H NMR spectrum of diamide **4** (Figure 5a). The fact that both signals are observed to shift simultaneously in the dilution and DMSO-d_6 addition studies

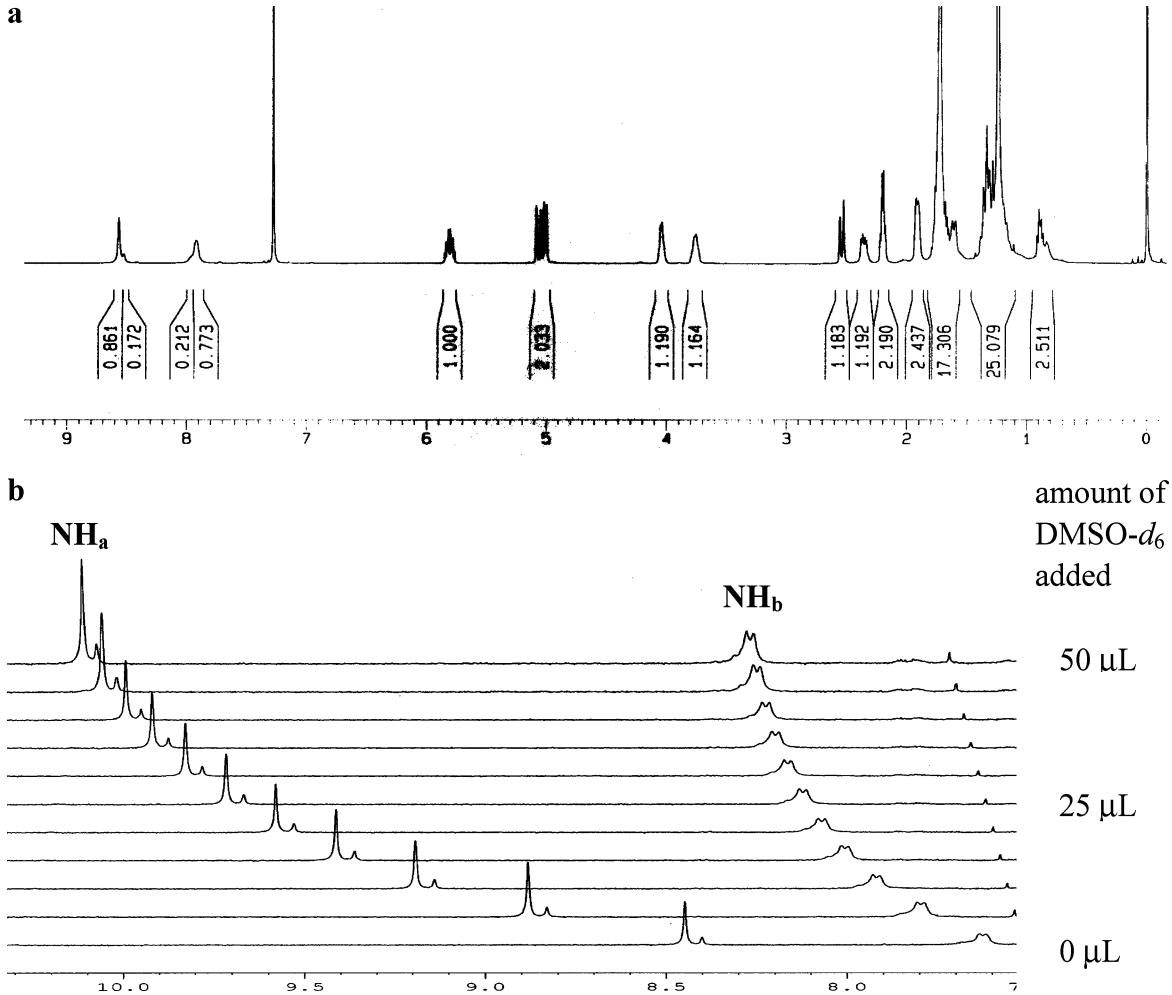

Figure 5. (a) The ^{1}H NMR spectrum of diamide **4** in $CDCl_3$ (5 mM at room temperature). (b) Overlaid ^{1}H NMR spectra of diamide **4** recorded during the DMSO-d_6 addition experiment. Starting from the foremost spectrum (5 mM solution in 0.5 mL of $CDCl_3$), 5 μL of DMSO-d_6 was added to the NMR tube before each successive spectrum was recorded at room temperature.

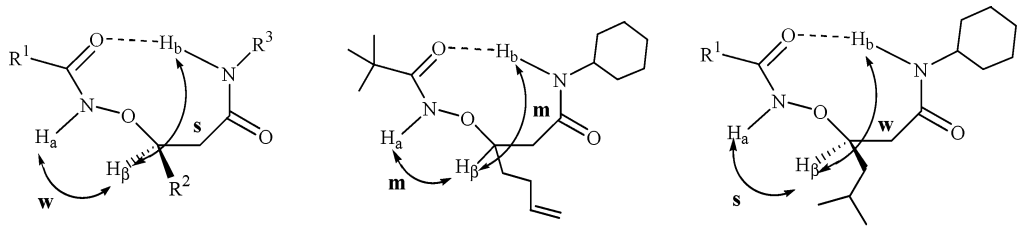

1 $R^2 = CH_3$
2 $R^2 = CH_2CH_3$
3 $R^2 = COOCH_2Ph$
7 $R^2 = CH(CH_3)_2$
8 $R^2 = CH(CH_3)_2$

4

5 $R^1 = (CH_3)_3CO$
6 $R^1 = (CH_3)_3C$

Figure 6. Summary of the NOEs observed (s, stronger NOE; m, medium NOE; w, weaker NOE) in the NOESY spectra of diamides **1**−**8** at 5 mM in $CDCl_3$ or CD_2Cl_2 at room temperature.

implies that they arise from two conformers, rather than from impurities, and the rate of exchange between the two conformers is slow enough for them to be distinguished by NMR spectroscopy (Figure 5b presents the DMSO-d_6 addition study as an example).[86]

2D-NOESY Studies of Diamides 1−8. We performed 2D-NOESY studies of diamides **1**−**8** in $CDCl_3$ or CD_2Cl_2 to probe their conformations in solution. The nuclear Overhauser effect (NOE) patterns observed for **1**−**3**, **7**, and **8** are distinct from those of **5** and **6** (Figure 6).[86] For **1**−**3**, **7**, and **8**, the NOE observed between protons H_a and H_β is weaker than that between H_b and H_β, with the NOE between protons H_b and H_β of **3** being particularly stronger than those of the others. In contrast, slightly stronger NOEs are observed between H_a and H_β than between H_b and H_β for **5** and **6**, and a medium/medium NOE pattern is observed for **4**.

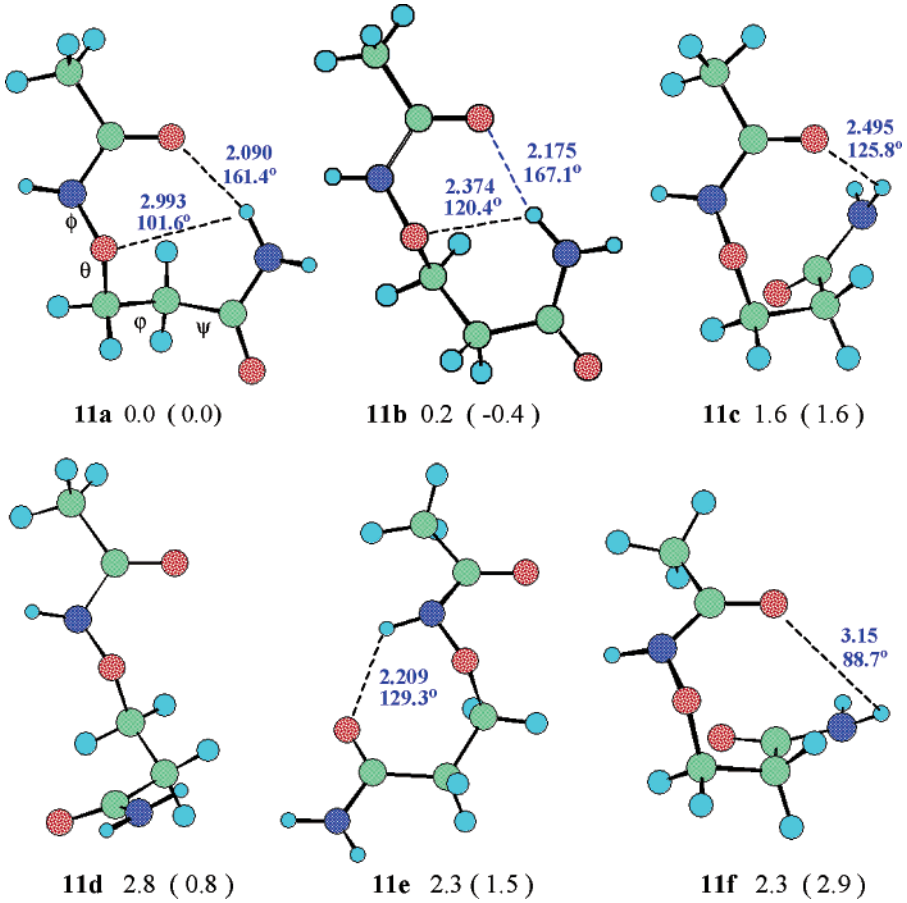

Figure 7. Calculated conformations of **11**. The relative free energies (kcal/mol) were calculated at the MP2/6-311G** level in the gas phase and in CH_2Cl_2 (in parentheses). The N−H···O hydrogen bond angles and the hydrogen bond distances (in angstroms) are indicated.

Theoretical Calculations. To understand the conformational features of compounds **1**−**8**, we carried out theoretical calculations on model systems **11**−**17**. All calculations were conducted

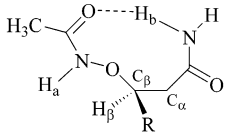

11 **12** **13** **14** **15** **16** **17**

R = H Me Et *i*-Pr *i*-Bu COOMe $CH_2CH_2CH{=}CH_2$

using the Gaussian 98 program,[87] except that in evaluating the solvent effects we used the Gaussian 94 program.[88] The geometry of each structure was fully optimized using the HF/6-31G** method, and then vibration frequency calculations were performed. Energies were evaluated using the B3LYP/6-311G** and MP2/6-311G** methods. Solvent effects were estimated from the SCIPCM model[89−91] using the B3LYP/6-311G** method.[92,93] The final relative energies of the different conformations were estimated by eq 1, which has been shown to be effective for other peptide systems:[78−81,94−97]

$$\Delta G = \Delta E(\mathrm{MP2}) + [\Delta E(\mathrm{B3LYP,\ solvent}) - \Delta E(\mathrm{B3LYP})] + \text{enthalpy correction} - T\Delta S \quad (1)$$

Figure 7 displays the six stable conformations of diamide **11**. Both structures **11a** and **11b** feature strong, nine-membered-ring, intramolecular hydrogen bonds, which are distinguished by their dihedral angles θ of ca. 85° in **11a** (gauche) and −173° in **11b** (anti). These two structures have similar stabilities. Structures **11c** and **11f** also possess nine-membered-ring hydrogen bonds, but they are much less stable because of severe

(87) Frisch, M. J.; Trucks, G. W.; Schlegel, H. B.; Scuseria, G. E.; Robb, M. A.; Cheeseman, J. R.; Zakrzewski, V. G.; Montgomery, J. A.; Stratmann, R. E.; Burant, J. C.; Dapprich, S.; Millam, J. M.; Daniels, A. D.; Kudin, K. N.; Strain, M. C.; Farkas, O.; Tomasi, J.; Barone, V.; Cossi, M.; Cammi, R.; Mennucci, B.; Pomelli, C.; Adamo, C.; Clifford, S.; Ochterski, J.; Petersson, G. A.; Ayala, P. Y.; Cui, Q.; Morokuma, K.; Malick, D. K.; Rabuck, A. D.; Raghavachari, K.; Foresman, J. B.; Cioslowski, J.; Oritz, J. V.; Stefanov, B. B.; Liu, G.; Liashenko, A.; Piskorz, P.; Komaromi, I.; Gomperts, R.; Martin, R. L.; Fox, D. J.; Keith, T.; Al-Laham, M. A.; Peng, C. Y.; Nanayakkara, A.; Gonzalez, C.; Challacombe, M.; Gill, P. M. W.; Johnson, B. G.; Chen, W.; Wong, M. W.; Andres, J. L.; Head-Gordon, M.; Replogle, E. S.; Pople, J. A. *Gaussian 98*, revision A.1; Gaussian, Inc.: Pittsburgh, PA, 1998.

(88) Frisch, M. J.; Trucks, G. W.; Schlegel, H. B.; Gill, P. M. W.; Johnson, B. G.; Robb, M. A.; Cheeseman, J. R.; Keith, T. A.; Petersson, G. A.; Montgomery, J. A.; Raghavachari, K.; Al-Laham, M. A.; Zakrzewski, V. G.; Ortiz, J. V.; Foresman, J. B.; Cioslowski, J.; Stefanov, B. B.; Nanayakkara, A.; Challacombe, M.; Peng, C. Y.; Ayala, P. Y.; Chen, W.; Wong, M. W.; Andres, J. L.; Replogle, E. S.; Gomperts, R.; Martin, R. L.; Fox, D. J.; Binkley, J. S.; Defrees, D. J.; Baker, J.; Stewart, J. P.; Head-Gordon, M.; Gonzalez, C.; Pople, J. A. *Gaussian 94*, revision B.3; Gaussian, Inc.: Pittsburgh, PA, 1995.

(89) Wiberg, K. B.; Keith, T. A.; Frisch, M. J.; Murcko, M. *J. Phys. Chem.* **1995**, *99*, 9072−9079.

(90) Foresman, J. B.; Keith, T. A.; Wiberg, K. B.; Snoonian, J.; Frisch, M. J. *J. Phys. Chem.* **1996**, *100*, 16098−16104.

(91) Tomasi, J.; Bonaccorsi, R. *Croat. Chem. Acta* **1992**, *65*, 29−54.

(92) Becke, A. D. *J. Chem. Phys.* **1993**, *98*, 5648−5652.

(93) Lee, C. T.; Yang, W. T.; Parr, R. G. *Phys. Rev. B* **1988**, *37*, 785−789.

(94) Zhao, Y. L.; Wu, Y. D. *J. Am. Chem. Soc.* **2002**, *124*, 1570−1571.

(95) Wu, Y. D.; Zhao, Y. L. *J. Am. Chem. Soc.* **2001**, *123*, 5313−5319.

(96) Wu, Y. D.; Wang, D. P. *J. Am. Chem. Soc.* **1999**, *121*, 9352−9362.

(97) Wu, Y. D.; Wang, D. P. *J. Am. Chem. Soc.* **1998**, *120*, 13485−13493.

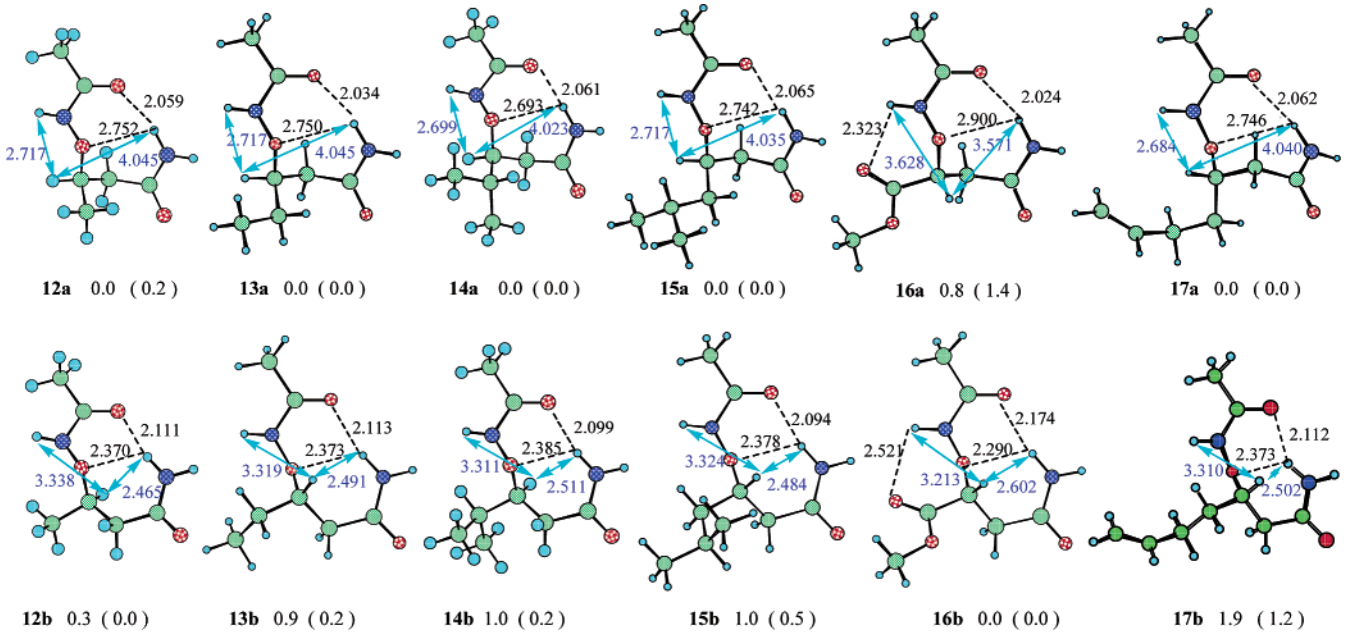

Figure 8. Calculated structures for the gauche and anti conformations of the nine-membered-ring structures of **12**−**17**. Relative energies (kcal/mol) were calculated at the MP2/6-311G** level in the gas phase and in CH_2Cl_2 solution (in parentheses). The H···H distances of the NH_a···$C_\beta H$ and NH_b···$C_\beta H$ interactions and the hydrogen bond distances of the NH_b···O interactions (in angstroms) are indicated.

geometrical distortions. Structure **11d** has an extended backbone and is ideal for the formation of sheet structures. It is ca. 2.6 and 1.2 kcal/mol less stable than **11b** in the gas phase and in CH_2Cl_2 solution, respectively. Structure **11e** has a seven-membered-ring hydrogen bond; we calculate it to be less stable in CH_2Cl_2 solution than **11b** by ca. 1.9 kcal/mol. The calculations, therefore, suggest that the dominant conformations of diamide **11** in CH_2Cl_2 solution are the two nine-membered-ring hydrogen-bonded conformations **11a** and **11b**. These two conformations can be readily interconverted by rotation about the O−C_β bond. This conformational feature of β-aminoxy peptides is quite different from that of analogous γ-peptides. Gellman et al. studied a diamide of a γ-peptide model (replacing the O atom in **11** by a CH_2 unit) and found that a nine-membered-ring hydrogen-bonded conformation and a seven-membered-ring hydrogen-bonded conformation are in equilibrium.[98] Theoretical calculations on the γ-diamide model indicated that a conformation similar to that of **11a** is the most stable one, but five other conformations were found that were only ca. 0.4−0.9 kcal/mol less stable in CH_2Cl_2 solution.[99] Thus, β-aminoxy peptides tend to form locally rigid conformations, whereas the analogous γ-peptides are much more flexible in their conformations.[71−75,100] This situation arises because the N−O bond is very rigid and the C−N−O−C_β unit has a strong preference to be perpendicular. This phenomenon also contributes significantly to the rigid conformational features of α-aminoxy peptides, which have a strong preference for an eight-membered-ring hydrogen-bonded local structure.[78−81]

Consequently, we focused our attention on calculations of the two nine-membered-ring conformations of the substituted diamide models **12**−**17**. Figure 8 displays the most stable conformations corresponding to **11a** and **11b** having a β^3-substituent.[101] The substituent does not change the overall geometry significantly. The calculated backbone dihedral angles are close to those found in the X-ray structures of **3** and **5**−**7**. Energetically, the methyl substituent has little effect on the preference between the two conformations: the gauche conformation **12a** is ca. 0.3 kcal/mol more stable than the anti conformation **12b** in the gas phase, but it is ca. 0.2 kcal/mol less stable than **12b** in CH_2Cl_2 solution, which is a finding that agrees well with the weak/strong NOE pattern observed for diamide **1**. When the methyl substituent is changed to an ethyl, isopropyl, or isobutyl group, we calculate the gauche conformation to be more stable than the anti conformation. This preference is larger in the gas phase than it is in solution. The calculated trends for the effects that substituents have on the conformational preferences can be applied to understand the experimental observations. In general, a bulky substituent causes destabilization of the anti conformation because the substituent in the anti conformation is in a more-crowded position. Solvent effects, on the other hand, favor the anti conformation. Experimentally, compounds **5**−**7** exist in gauche conformations in the solid state. The results of calculations in the gas phase do indicate a considerable preference for the gauche conformations **13a** and **14a** over the anti conformations **13b** and **14b**, respectively. In solution, however, the calculations indicate that **13a** and **14a** are only ca. 0.2 kcal/mol more stable than **13b** and **14b**, respectively. We note that, in **13a** and **14a**, the NH_a···$C_\beta H$ distance is ca. 2.7 Å, while in **13b** and **14b** the NH_b···$C_\beta H$ distance is ca. 2.5 Å. If the anti and gauche conformations are equally distributed, we would expect a weak NOE for the NH_a···$C_\beta H$ interaction and a stronger one for NH_b···$C_\beta H$. This rationale seems to be in agreement with the NOE patterns observed for diamides **2**, **7**, and **8**. Calculations suggest a larger

(98) Dado, G. P.; Gellman, S. H. *J. Am. Chem. Soc.* **1994**, *116*, 1054−1062. Actually, their experiment used the *N*-methylated diamide; we expect that this methylation has little effect on the conformational features.

(99) (a) The work was presented at the 219th ACS meeting in San Francisco, CA, 2000. Zhao, Y.-L.; Wu, Y.-D. Abstract for ACS meeting. (b) Zhao, Y.-L. Ph.D. Thesis, The Hong Kong University of Science & Technology, 2002.

(100) Brenner, M.; Seebach, D. *Helv. Chim. Acta* **2001**, *84*, 1181−1189.

(101) In the cases of **12**−**17**, we calculated many possible conformations for the side chains. For detailed information, see the Supporting Information.

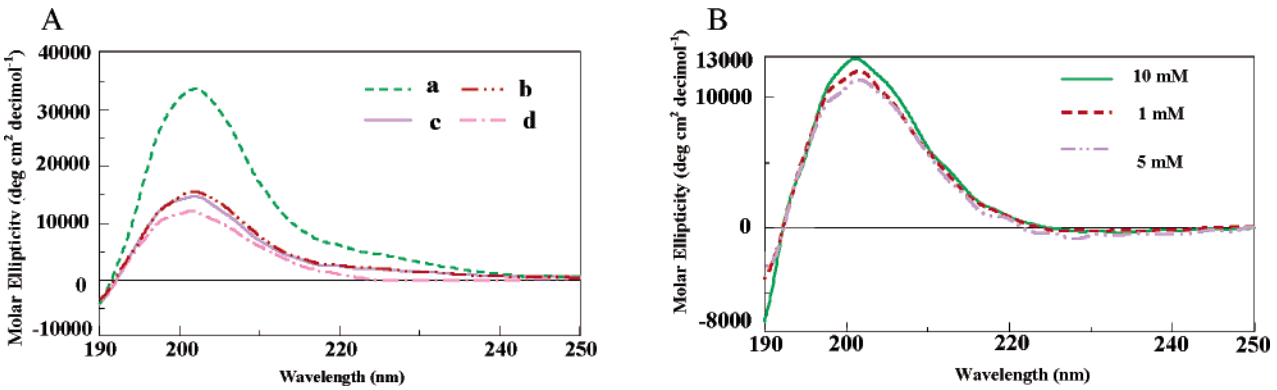

Figure 9. (A) Circular dichroism spectra of diamides **1**, **2**, and **6** recorded from 1 mM solutions at room temperature. (a) **6** in MeCN; (b) **2** in MeCN; (c) **1** in MeCN; (d) **2** in CF_3CH_2OH. (B) Circular dichroism spectra of different concentrations of diamide **2** in CF_3CH_2OH recorded at room temperature. The spectra have been normalized for the concentration of the compounds.

preference for the gauche conformation **15a** over the anti conformation **15b**. This result explains the differences in the NOE patterns observed between diamides **6** and **2**.[102]

In the case of **16**, calculations indicate that the side-chain ester group is involved in a hydrogen bond with the NH_a group in both the anti and the gauche conformations. In this case, the anti conformation (**16b**) is considerably more stable than the gauche conformation (**16a**), by ca. 0.8 and 1.4 kcal/mol in the gas phase and in CH_2Cl_2 solution, respectively. This calculation is in good agreement with the solid-state structure (Figure 4) and the experimental observation that the NOE between the NH_b and $C_\beta H$ protons of diamide **3** is obviously strong. In the gauche conformation, both the $C_\beta-C_\alpha$ and the $C_\beta-C_\gamma$ bonds are gauche to the N−O bond, which is destabilized sterically.

Calculations on **17** reveal that the gauche conformation is much more stable than the anti conformation. Thus, the homoallyl group behaves as a sterically "larger" group than the isopropyl and isobutyl groups. To understand this finding, we note that there is a strong tendency for the vinyl substituent to be gauche with respect to the $C_\beta-C_\gamma$ bond. This conformational preference is likely to be caused by an electrostatic attraction between the vinyl group and the positively charged $C_\beta H$ group. Such an interaction appears to be more effective in the gauche conformation (**17a**) than it is in the anti one (**17b**).

CD Studies of Diamides 1, 2, and 6. Circular dichroism (CD) spectroscopy has been used successfully to characterize the secondary structures of α-peptides,[7−9,30,103,104] β-peptides,[38,56,60,67] γ-peptides,[75] and other unnatural oligomers.[105−107] We used CD spectroscopy as an additional tool to probe the conformations of the homochiral oligomers of β^3-aminoxy acids. Figure 9A presents the overlaid spectra of the diamides having different side chains. Diamide **2** exhibits a slightly different absorption in two different solvents, CF_3CH_2OH and MeCN. In CF_3CH_2OH, the curve for **2** is observed having a maximum at ca. 202 nm, a minimum at ca. 237 nm, and zero crossing at 224 nm, which is very similar to those traces observed for α-aminoxy peptides, albeit with a slight blue-shift (maxima at ca. 195 nm).[80] The CD curves of **2** changed little when the concentration was increased from 1 to 10 mM, which indicates that there was no aggregation (Figure 9B). Changing the solvent for **2** from CF_3CH_2OH to MeCN led to a slight increase in the intensity, and the negative minimum disappeared. The CD spectra of diamides **1** and **6** in CF_3CH_2OH could not be determined because of their poor solubilities. In MeCN, however, the CD spectra of **1** and **6** are similar to those of **2** with maxima at ca. 200 nm, although the intensity of **6** was significantly higher than that of either **1** or **2**. This observation indicates that the gauche conformation of **6** is more favorable in solution, whereas anti conformations might predominate for **1** and **2**. This conclusion is in agreement with the results of the above calculations.

Two Types of β N−O Helices Induced by β^3-Aminoxy Peptides. Because there are two types of β N−O turns induced by β^3-aminoxy acids, we used triamides **9** and **10**, which have small (methyl) and large (isobutyl) side chains, respectively, to probe the effect that the side chains have on the helical conformations of β^3-aminoxy peptides.

A dilution study of triamide **10** (from 200 to 1 mM), monitored by ^{1}H NMR spectroscopy, indicates that the chemical shifts of the amide protons, except that of the NH_a unit at the N-terminus, were independent of the concentration.[86] A similar study of triamide **9** could not be performed because of its poor solubility in $CDCl_3$. Nevertheless, the dramatic downfield shifts ($\Delta\delta$ > 2.26 ppm) observed by ^{1}H NMR spectroscopy for the NH_a protons relative to the NH_b and NH_c protons ($\Delta\delta$ < 0.34 ppm) in the DMSO-d_6 addition studies of both **9** and **10** suggest that the protons of the *N*-oxy amide NH_b and regular amide NH_c groups are intramolecularly hydrogen-bonded, but the N-terminal NH_a groups are not.[86] Four peaks are observed in the N−H stretching region of the IR spectra of both **9** and **10** (Figure 10); they correspond to hydrogen-bonded NH_b (3192 and 3234 cm^{-1}, respectively), hydrogen-bonded NH_c (3287 and 3289 cm^{-1}, respectively), non-hydrogen-bonded NH_a (3387 and 3354 cm^{-1}, respectively), and non-hydrogen-bonded NH_c (3430 and 3446 cm^{-1}, respectively) units. The small peaks at 3430 and 3446 cm^{-1} indicate that only negligible concentrations of

(102) Calculations based on the Boltzman distribution of all of the conformations considered give the following anti:gauche ratios at 298 K: R_2 = Me (**12**), 1.4:1; R_2 = Et (**13**), 1:1.2; R_2 = *i*-Pr (**14**), 1:1.3; R_2 = *i*-Bu (**15**), 1:2.8; R_2 = COOMe (**16**), 17.1:1; R_2 = $CH_2CH_2CH{=}CH_2$ (**17**), 1:4.1. In the case of **17**, another conformation corresponding to rotation of the vinyl group in **17b** by ca. 180° has about the same stability as **17b** (see the Supporting Information, Table S9).

(103) Lu, H. S. M.; Volk, M.; Kholodenko, Y.; Gooding, E.; Hochstrasser, R. M.; DeGrado, W. F. *J. Am. Chem. Soc.* **1997**, *119*, 7173−7180.
(104) Albert, J. S.; Peczuh, M. W.; Hamilton, A. D. *Bioorg. Med. Chem.* **1997**, *5*, 1455−1467.
(105) Szabo, L.; Smith, B. L.; McReynolds, K. D.; Parrill, A. L.; Morris, E. R.; Gervay, J. *J. Org. Chem.* **1998**, *63*, 1074−1078.
(106) Gin, M. S.; Moore, J. S. *Org. Lett.* **2000**, *2*, 135−138.
(107) Yu, M.; Nowak, A. P.; Deming, T. J.; Pochan, D. J. *J. Am. Chem. Soc.* **1999**, *121*, 12210−12211.

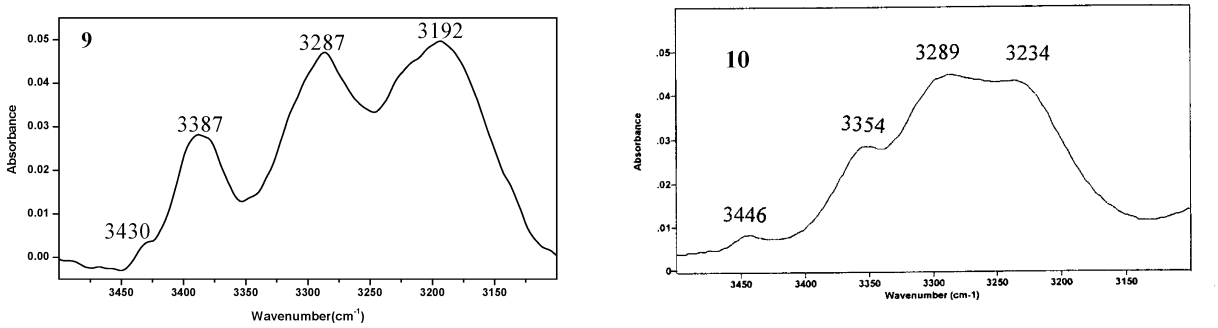

Figure 10. The N−H stretching region of FTIR spectra of triamides **9** and **10** at 1 mM in CH_2Cl_2 recorded at room temperature, after subtraction of the spectrum of pure CH_2Cl_2.

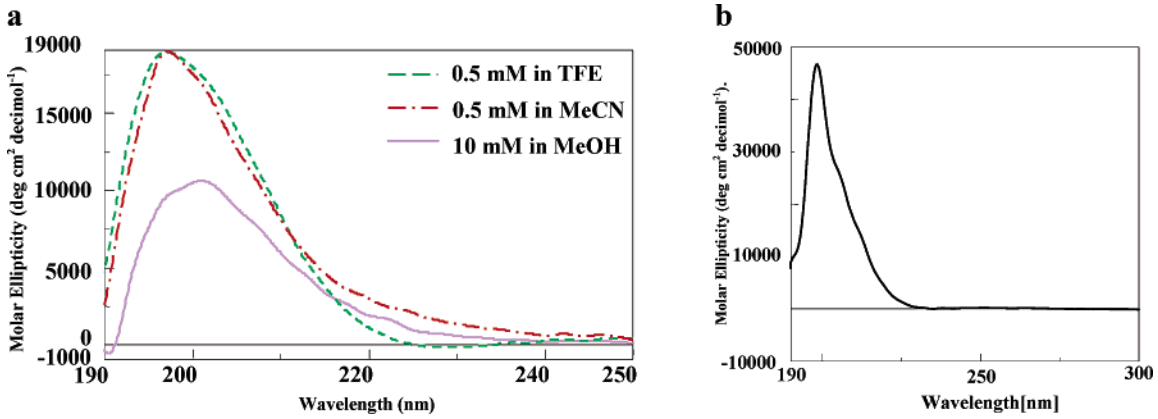

Figure 11. (a) The CD spectra of triamide **9** in different solvents recorded at room temperature. (b) The CD spectrum of triamide **10** (0.5 mM) in TFE recorded at room temperature. All of the CD data have been normalized for the concentration of the compound and the number of backbone N−O turns.

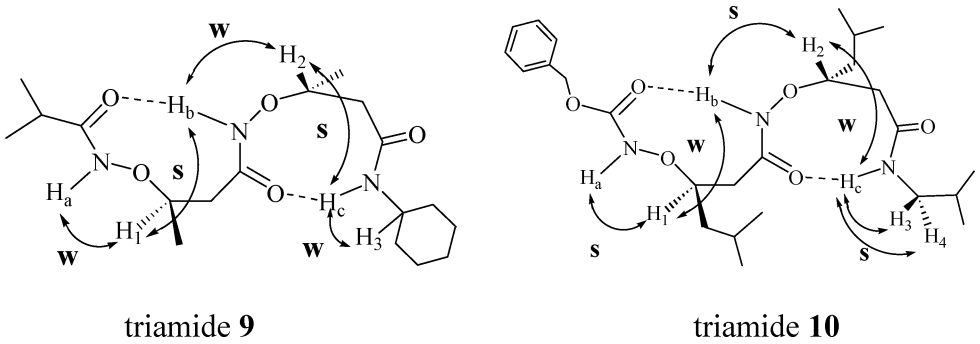

Figure 12. Summary of the NOEs observed (s, stronger NOE; w, weaker NOE) for triamides **9** and **10** at 5 mM in $CDCl_3$ at room temperature.

the non-hydrogen-bonded conformations of both **9** and **10** are present in CH_2Cl_2.

We observe a unique absorption in the CD spectra of triamide **9** in CF_3CH_2OH, MeCN, and MeOH with a maximum at ca. 198 nm (Figure 11a). The shape of the curve is similar to that of the CD spectrum of diamide **1** (Figure 9A), but the maximum is slightly red-shifted. In MeOH, the CD absorption is slightly less intense than it is in MeCN or CF_3CH_2OH, which is a finding that is similar to the features of the 1.8_8-helix observed in peptides of homochiral α-aminoxy acids.[80] Triamide **10** exhibits a maximum at 198.5 nm (Figure 11b), which is almost the same as that of **9** except that the intensity has increased significantly; these findings are in agreement with the fact that the intensity of diamide **6** (Figure 9A) is much higher than that of diamide **1**. Therefore, a helical structure having two nine-membered-ring hydrogen bonds, that is, two consecutive β N−O turns, is formed in both **9** and **10**. In addition, these helices are stable enough to be observed, even in a polar solvent such as methanol.

Interestingly, two different NOE patterns are also observed for triamides **9** and **10** (Figure 12) that are analogous to those observed in the β N−O turns of diamides. Therefore, two types of β N−O helix built from two types of β N−O turns are dominant in **9** and **10**. The N−O bond is anti to the $C_\alpha-C_\beta$ bond in **9**, which features methyl side chains, but it is gauche in **10**, which has isobutyl side chains.

X-ray Crystallographic Analysis of the Sheet Structures of 1 and 9 in the Solid State. The studies above indicate that, in solution, the diamides **1**−**8** adopt β N−O turn conformations and the triamides **9** and **10** exist in β N−O helices. These findings were also confirmed by the solid-state structures of **3** and **5**−**7** (Figure 4). Surprisingly, the solid-state conformations of **1** and **9** turned out to be different. Rather than a turn or a helix, **1** and **9** exist in the solid state in more-extended sheetlike structures having intermolecular hydrogen bonds (Figure 13). The backbone torsional angles of diamide **1** and triamide **9** in their solid-state structures are summarized in Table 2. In these

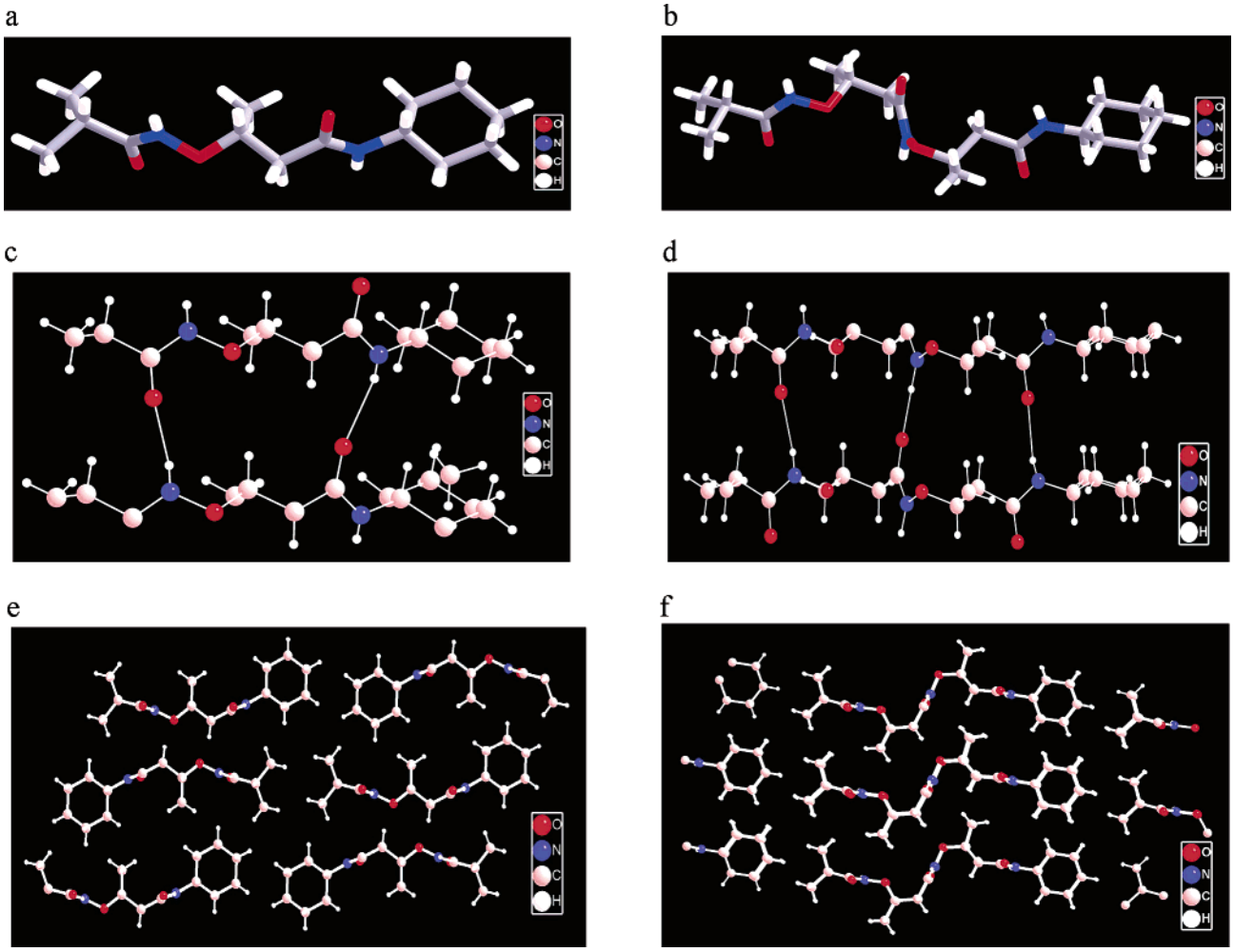

Figure 13. The solid-state structures of (a) diamide **1** and (b) triamide **9**. The parallel sheet structures present in the packing of (c) diamide **1** and (d) triamide **9** in the solid state. Plan views of the solid-state packing of (e) diamide **1** and (f) triamide **9**.

Table 2. Torsional Angles of Diamide **1** and Triamide **9** in Their Solid-State Structures

compound	ϕ	θ	φ	ψ
1	126.77°	172.46°	−173.91°	−120.60°
9	127.78°	172.41°	−59.74°	118.16°
	−116.57°	63.55°	−171.18°	−141.16°

extended conformations, all of the amide groups are involved in intermolecular 16-membered-ring hydrogen bonding in a parallel fashion. According to the results of calculations (Figure 7), although **11d** is less stable than the other conformations, the difference between them in energy is not too great. For **1** and **9**, which have small side chains, it seems possible that hydrophobic interactions between the protecting groups at both the C- and the N-termini cause the existence of sheet structures to be more favorable in the solid state where the molecules are packed at exceedingly "high concentration".

Conclusion

We have presented our studies on the conformational preferences of β^3-aminoxy peptides, which are a new subclass of β-aminoxy peptides. Both experimental studies and theoretical calculations on β N−O turns and β N−O helices in β^3-aminoxy peptides have provided much insight into the nature of the folding of β-aminoxy peptides. The N−O bond in the β^3-aminoxy peptides can be either anti or gauche to the C_α−C_β bond depending on the size of the side chain on the β-carbon atom, whereas only the anti conformation was found to be present in $\beta^{2,2}$-aminoxy peptides. Moreover, we discovered that some differences occur between the conformations in solution and those existing in the solid state. Understanding the effects that the side chains have on local conformational features should stimulate the design of new foldamers.

Acknowledgment. This work was supported by The University of Hong Kong and Research Grants Council of Hong Kong. D.Y. acknowledges the Bristol-Myers Squibb Foundation for an Unrestricted Grant in Synthetic Organic Chemistry and the Croucher Foundation for a Croucher Senior Research Fellowship Award.

Supporting Information Available: Characterization data for **1**−**10**; ^{1}H NMR spectroscopic data for the dilution and DMSO-d_6 addition experiments of **1**−**5**, **7**, **9** and **10**; 2D-NOESY spectra of **1**−**10**; X-ray crystallographic structural analyses of **1**, **3**, **5**−**7**, and **9**, including tables of bond lengths and angles (PDF); X-ray crystallographic file (CIF); tables of calculated energies and structures of compounds **11**−**17** and Cartesian coordinates of the structures (PDF). This material is available free of charge via the Internet at http://pubs.acs.org.

JA049976S